Measurement of the W boson mass

V.M. Abazov[37], B. Abbott[75], M. Abolins[65], B.S. Acharya[30], M. Adams[51], T. Adams[49], E. Aguilo[6], M. Ahsan[59], G.D. Alexeev[37], G. Alkhazov[41], A. Alton[64,a], G. Alverson[63], G.A. Alves[2], L.S. Ancu[36], T. Andeen[53], M.S. Anzelc[53], M. Aoki[50], Y. Arnoud[14], M. Arov[60], M. Arthaud[18], A. Askew[49,b], B. Åsman[42], O. Atramentov[49,b], C. Avila[8], J. BackusMayes[82], F. Badaud[13], L. Bagby[50], B. Baldin[50], D.V. Bandurin[59], S. Banerjee[30], E. Barberis[63], A.-F. Barfuss[15], P. Bargassa[80], P. Baringer[58], J. Barreto[2], J.F. Bartlett[50], U. Bassler[18], D. Bauer[44], S. Beale[6], A. Bean[58], M. Begalli[3], M. Begel[73], C. Belanger-Champagne[42], L. Bellantoni[50], A. Bellavance[50], J.A. Benitez[65], S.B. Beri[28], G. Bernardi[17], R. Bernhard[23], I. Bertram[43], M. Besançon[18], R. Beuselinck[44], V.A. Bezzubov[40], P.C. Bhat[50], V. Bhatnagar[28], G. Blazey[52], S. Blessing[49], K. Bloom[67], A. Boehnlein[50], D. Boline[62], T.A. Bolton[59], E.E. Boos[39], G. Borissov[43], T. Bose[62], A. Brandt[78], R. Brock[65], G. Brooijmans[70], A. Bross[50], D. Brown[19], X.B. Bu[7], D. Buchholz[53], M. Buehler[81], V. Buescher[22], V. Bunichev[39], S. Burdin[43,c], T.H. Burnett[82], C.P. Buszello[44], P. Calfayan[26], B. Calpas[15], S. Calvet[16], J. Cammin[71], M.A. Carrasco-Lizarraga[34], E. Carrera[49], W. Carvalho[3], B.C.K. Casey[50], H. Castilla-Valdez[34], S. Chakrabarti[72], D. Chakraborty[52], K.M. Chan[55], A. Chandra[48], E. Cheu[46], D.K. Cho[62], S.W. Cho[32], S. Choi[33], B. Choudhary[29], T. Christoudias[44], S. Cihangir[50], D. Claes[67], J. Clutter[58], M. Cooke[50], W.E. Cooper[50], M. Corcoran[80], F. Couderc[18], M.-C. Cousinou[15], D. Cutts[77], M. Ćwiok[31], A. Das[46], G. Davies[44], K. De[78], S.J. de Jong[36], E. De La Cruz-Burelo[34], K. DeVaughan[67], F. Déliot[18], M. Demarteau[50], R. Demina[71], D. Denisov[50], S.P. Denisov[40], S. Desai[50], H.T. Diehl[50], M. Diesburg[50], A. Dominguez[67], T. Dorland[82], A. Dubey[29], L.V. Dudko[39], L. Duflot[16], D. Duggan[49], A. Duperrin[15], S. Dutt[28], A. Dyshkant[52], M. Eads[67], D. Edmunds[65], J. Ellison[48], V.D. Elvira[50], Y. Enari[77], S. Eno[61], M. Escalier[15], H. Evans[54], A. Evdokimov[73], V.N. Evdokimov[40], G. Facini[63], A.V. Ferapontov[59], T. Ferbel[61,71], F. Fiedler[25], F. Filthaut[36], W. Fisher[50], H.E. Fisk[50], M. Fortner[52], H. Fox[43], S. Fu[50], S. Fuess[50], T. Gadfort[70], C.F. Galea[36], A. Garcia-Bellido[71], V. Gavrilov[38], P. Gay[13], W. Geist[19], W. Geng[15,65], C.E. Gerber[51], Y. Gershtein[49,b], D. Gillberg[6], G. Ginther[50,71], B. Gómez[8], A. Goussiou[82], P.D. Grannis[72], S. Greder[19], H. Greenlee[50], Z.D. Greenwood[60], E.M. Gregores[4], G. Grenier[20], Ph. Gris[13], J.-F. Grivaz[16], A. Grohsjean[18], S. Grünendahl[50], M.W. Grünewald[31], F. Guo[72], J. Guo[72], G. Gutierrez[50], P. Gutierrez[75], A. Haas[70], P. Haefner[26], S. Hagopian[49], J. Haley[68], I. Hall[65], R.E. Hall[47], L. Han[7], K. Harder[45], A. Harel[71], J.M. Hauptman[57], J. Hays[44], T. Hebbeker[21], D. Hedin[52], J.G. Hegeman[35], A.P. Heinson[48], U. Heintz[62], C. Hensel[24], I. Heredia-De La Cruz[34], K. Herner[64], G. Hesketh[63], M.D. Hildreth[55], R. Hirosky[81], T. Hoang[49], J.D. Hobbs[72], B. Hoeneisen[12], M. Hohlfeld[22], S. Hossain[75], P. Houben[35], Y. Hu[72], Z. Hubacek[10], N. Huske[17], V. Hynek[10], I. Iashvili[69], R. Illingworth[50], A.S. Ito[50], S. Jabeen[62], M. Jaffré[16], S. Jain[75], K. Jakobs[23], D. Jamin[15], R. Jesik[44], K. Johns[46], C. Johnson[70], M. Johnson[50], D. Johnston[67], A. Jonckheere[50], P. Jonsson[44], A. Juste[50], E. Kajfasz[15], D. Karmanov[39], P.A. Kasper[50], I. Katsanos[67], V. Kaushik[78], R. Kehoe[79], S. Kermiche[15], N. Khalatyan[50], A. Khanov[76], A. Kharchilava[69], Y.N. Kharzheev[37], D. Khatidze[77], M.H. Kirby[53], M. Kirsch[21], B. Klima[50], J.M. Kohli[28], J.-P. Konrath[23], A.V. Kozelov[40], J. Kraus[65], T. Kuhl[25], A. Kumar[69], A. Kupco[11], T. Kurča[20], V.A. Kuzmin[39], J. Kvita[9], F. Lacroix[13], D. Lam[55], S. Lammers[54], G. Landsberg[77], P. Lebrun[20], H.S. Lee[32], W.M. Lee[50], A. Leflat[39], J. Lellouch[17], L. Li[48], Q.Z. Li[50], S.M. Lietti[5], J.K. Lim[32], D. Lincoln[50], J. Linnemann[65], V.V. Lipaev[40], R. Lipton[50], Y. Liu[7], Z. Liu[6], A. Lobodenko[41], M. Lokajicek[11], P. Love[43], H.J. Lubatti[82], R. Luna-Garcia[34,d], A.L. Lyon[50], A.K.A. Maciel[2], D. Mackin[80], P. Mättig[27], R. Magaña-Villalba[34], P.K. Mal[46], S. Malik[67], V.L. Malyshev[37], Y. Maravin[59], B. Martin[14], R. McCarthy[72], C.L. McGivern[58], M.M. Meijer[36], A. Melnitchouk[66], L. Mendoza[8], D. Menezes[52], P.G. Mercadante[5], M. Merkin[39], K.W. Merritt[50], A. Meyer[21], J. Meyer[24], N.K. Mondal[30], H.E. Montgomery[50], R.W. Moore[6], T. Moulik[58], G.S. Muanza[15], M. Mulhearn[70], O. Mundal[22], L. Mundim[3], E. Nagy[15], M. Naimuddin[50], M. Narain[77], H.A. Neal[64], J.P. Negret[8], P. Neustroev[41], H. Nilsen[23], H. Nogima[3], S.F. Novaes[5], T. Nunnemann[26], G. Obrant[41], C. Ochando[16], D. Onoprienko[59], J. Orduna[34], N. Oshima[50], N. Osman[44], J. Osta[55], R. Otec[10], G.J. Otero y Garzón[1], M. Owen[45], M. Padilla[48], P. Padley[80], M. Pangilinan[77], N. Parashar[56], S.-J. Park[24], S.K. Park[32], J. Parsons[70], R. Partridge[77], N. Parua[54], A. Patwa[73], B. Penning[23], M. Perfilov[39], K. Peters[45], Y. Peters[45], P. Pétroff[16], R. Piegaia[1], J. Piper[65], M.-A. Pleier[22], P.L.M. Podesta-Lerma[34,e], V.M. Podstavkov[50], Y. Pogorelov[55], M.-E. Pol[2], P. Polozov[38], A.V. Popov[40], M. Prewitt[80], S. Protopopescu[73], J. Qian[64], A. Quadt[24], B. Quinn[66], A. Rakitine[43], M.S. Rangel[16], K. Ranjan[29], P.N. Ratoff[43], P. Renkel[79], P. Rich[45], M. Rijssenbeek[72], I. Ripp-Baudot[19], F. Rizatdinova[76], S. Robinson[44], M. Rominsky[75], C. Royon[18], P. Rubinov[50], R. Ruchti[55], G. Safronov[38], G. Sajot[14],

A. Sánchez-Hernández[34], M.P. Sanders[26], B. Sanghi[50], G. Savage[50], L. Sawyer[60], T. Scanlon[44], D. Schaile[26], R.D. Schamberger[72], Y. Scheglov[41], H. Schellman[53], T. Schliephake[27], S. Schlobohm[82], C. Schwanenberger[45], R. Schwienhorst[65], J. Sekaric[49], H. Severini[75], E. Shabalina[24], M. Shamim[59], V. Shary[18], A.A. Shchukin[40], R.K. Shivpuri[29], V. Siccardi[19], V. Simak[10], V. Sirotenko[50], P. Skubic[75], P. Slattery[71], D. Smirnov[55], G.R. Snow[67], J. Snow[74], S. Snyder[73], S. Söldner-Rembold[45], L. Sonnenschein[21], A. Sopczak[43], M. Sosebee[78], K. Soustruznik[9], B. Spurlock[78], J. Stark[14], V. Stolin[38], D.A. Stoyanova[40], J. Strandberg[64], M.A. Strang[69], E. Strauss[72], M. Strauss[75], R. Ströhmer[26], D. Strom[51], L. Stutte[50], S. Sumowidagdo[49], P. Svoisky[36], M. Takahashi[45], A. Tanasijczuk[1], W. Taylor[6], B. Tiller[26], M. Titov[18], V.V. Tokmenin[37], I. Torchiani[23], D. Tsybychev[72], B. Tuchming[18], C. Tully[68], P.M. Tuts[70], R. Unalan[65], L. Uvarov[41], S. Uvarov[41], S. Uzunyan[52], P.J. van den Berg[35], R. Van Kooten[54], W.M. van Leeuwen[35], N. Varelas[51], E.W. Varnes[46], I.A. Vasilyev[40], P. Verdier[20], L.S. Vertogradov[37], M. Verzocchi[50], M. Vesterinen[45], D. Vilanova[18], P. Vint[44], P. Vokac[10], R. Wagner[68], H.D. Wahl[49], M.H.L.S. Wang[71], J. Warchol[55], G. Watts[82], M. Wayne[55], G. Weber[25], M. Weber[50,f], L. Welty-Rieger[54], A. Wenger[23,g], M. Wetstein[61], A. White[78], D. Wicke[25], M.R.J. Williams[43], G.W. Wilson[58], S.J. Wimpenny[48], M. Wobisch[60], D.R. Wood[63], T.R. Wyatt[45], Y. Xie[77], C. Xu[64], S. Yacoob[53], R. Yamada[50], W.-C. Yang[45], T. Yasuda[50], Y.A. Yatsunenko[37], Z. Ye[50], H. Yin[7], K. Yip[73], H.D. Yoo[77], S.W. Youn[50], J. Yu[78], C. Zeitnitz[27], S. Zelitch[81], T. Zhao[82], B. Zhou[64], J. Zhu[72], M. Zielinski[71], D. Zieminska[54], L. Zivkovic[70], V. Zutshi[52], and E.G. Zverev[39]

(The DØ Collaboration)

[1]Universidad de Buenos Aires, Buenos Aires, Argentina
[2]LAFEX, Centro Brasileiro de Pesquisas Físicas, Rio de Janeiro, Brazil
[3]Universidade do Estado do Rio de Janeiro, Rio de Janeiro, Brazil
[4]Universidade Federal do ABC, Santo André, Brazil
[5]Instituto de Física Teórica, Universidade Estadual Paulista, São Paulo, Brazil
[6]University of Alberta, Edmonton, Alberta, Canada; Simon Fraser University,
Burnaby, British Columbia, Canada; York University, Toronto,
Ontario, Canada and McGill University, Montreal, Quebec, Canada
[7]University of Science and Technology of China, Hefei, People's Republic of China
[8]Universidad de los Andes, Bogotá, Colombia
[9]Center for Particle Physics, Charles University,
Faculty of Mathematics and Physics, Prague, Czech Republic
[10]Czech Technical University in Prague, Prague, Czech Republic
[11]Center for Particle Physics, Institute of Physics,
Academy of Sciences of the Czech Republic, Prague, Czech Republic
[12]Universidad San Francisco de Quito, Quito, Ecuador
[13]LPC, Université Blaise Pascal, CNRS/IN2P3, Clermont, France
[14]LPSC, Université Joseph Fourier Grenoble 1, CNRS/IN2P3,
Institut National Polytechnique de Grenoble, Grenoble, France
[15]CPPM, Aix-Marseille Université, CNRS/IN2P3, Marseille, France
[16]LAL, Université Paris-Sud, IN2P3/CNRS, Orsay, France
[17]LPNHE, IN2P3/CNRS, Universités Paris VI and VII, Paris, France
[18]CEA, Irfu, SPP, Saclay, France
[19]IPHC, Université de Strasbourg, CNRS/IN2P3, Strasbourg, France
[20]IPNL, Université Lyon 1, CNRS/IN2P3, Villeurbanne, France and Université de Lyon, Lyon, France
[21]III. Physikalisches Institut A, RWTH Aachen University, Aachen, Germany
[22]Physikalisches Institut, Universität Bonn, Bonn, Germany
[23]Physikalisches Institut, Universität Freiburg, Freiburg, Germany
[24]II. Physikalisches Institut, Georg-August-Universität Göttingen, Göttingen, Germany
[25]Institut für Physik, Universität Mainz, Mainz, Germany
[26]Ludwig-Maximilians-Universität München, München, Germany
[27]Fachbereich Physik, University of Wuppertal, Wuppertal, Germany
[28]Panjab University, Chandigarh, India
[29]Delhi University, Delhi, India
[30]Tata Institute of Fundamental Research, Mumbai, India
[31]University College Dublin, Dublin, Ireland
[32]Korea Detector Laboratory, Korea University, Seoul, Korea
[33]SungKyunKwan University, Suwon, Korea
[34]CINVESTAV, Mexico City, Mexico
[35]FOM-Institute NIKHEF and University of Amsterdam/NIKHEF, Amsterdam, The Netherlands
[36]Radboud University Nijmegen/NIKHEF, Nijmegen, The Netherlands
[37]Joint Institute for Nuclear Research, Dubna, Russia

[38]Institute for Theoretical and Experimental Physics, Moscow, Russia

[39]Moscow State University, Moscow, Russia

[40]Institute for High Energy Physics, Protvino, Russia

[41]Petersburg Nuclear Physics Institute, St. Petersburg, Russia

[42]Stockholm University, Stockholm, Sweden, and Uppsala University, Uppsala, Sweden

[43]Lancaster University, Lancaster, United Kingdom

[44]Imperial College, London, United Kingdom

[45]University of Manchester, Manchester, United Kingdom

[46]University of Arizona, Tucson, Arizona 85721, USA

[47]California State University, Fresno, California 93740, USA

[48]University of California, Riverside, California 92521, USA

[49]Florida State University, Tallahassee, Florida 32306, USA

[50]Fermi National Accelerator Laboratory, Batavia, Illinois 60510, USA

[51]University of Illinois at Chicago, Chicago, Illinois 60607, USA

[52]Northern Illinois University, DeKalb, Illinois 60115, USA

[53]Northwestern University, Evanston, Illinois 60208, USA

[54]Indiana University, Bloomington, Indiana 47405, USA

[55]University of Notre Dame, Notre Dame, Indiana 46556, USA

[56]Purdue University Calumet, Hammond, Indiana 46323, USA

[57]Iowa State University, Ames, Iowa 50011, USA

[58]University of Kansas, Lawrence, Kansas 66045, USA

[59]Kansas State University, Manhattan, Kansas 66506, USA

[60]Louisiana Tech University, Ruston, Louisiana 71272, USA

[61]University of Maryland, College Park, Maryland 20742, USA

[62]Boston University, Boston, Massachusetts 02215, USA

[63]Northeastern University, Boston, Massachusetts 02115, USA

[64]University of Michigan, Ann Arbor, Michigan 48109, USA

[65]Michigan State University, East Lansing, Michigan 48824, USA

[66]University of Mississippi, University, Mississippi 38677, USA

[67]University of Nebraska, Lincoln, Nebraska 68588, USA

[68]Princeton University, Princeton, New Jersey 08544, USA

[69]State University of New York, Buffalo, New York 14260, USA

[70]Columbia University, New York, New York 10027, USA

[71]University of Rochester, Rochester, New York 14627, USA

[72]State University of New York, Stony Brook, New York 11794, USA

[73]Brookhaven National Laboratory, Upton, New York 11973, USA

[74]Langston University, Langston, Oklahoma 73050, USA

[75]University of Oklahoma, Norman, Oklahoma 73019, USA

[76]Oklahoma State University, Stillwater, Oklahoma 74078, USA

[77]Brown University, Providence, Rhode Island 02912, USA

[78]University of Texas, Arlington, Texas 76019, USA

[79]Southern Methodist University, Dallas, Texas 75275, USA

[80]Rice University, Houston, Texas 77005, USA

[81]University of Virginia, Charlottesville, Virginia 22901, USA and

[82]University of Washington, Seattle, Washington 98195, USA

(Dated: August 5, 2009)

We present a measurement of the W boson mass in $W \to e\nu$ decays using $1~\text{fb}^{-1}$ of data collected with the D0 detector during Run II of the Fermilab Tevatron collider. With a sample of 499830 $W \to e\nu$ candidate events, we measure $M_W = 80.401 \pm 0.043$ GeV. This is the most precise measurement from a single experiment.

Knowledge of the W boson mass (M_W) is currently a limiting factor in our ability to tighten the constraints on the mass of the Higgs boson as determined from internal consistency of the standard model (SM) [1]. Improving the measurement of M_W is an important contribution to our understanding of the electroweak (EW) interaction, and, potentially, of how the electroweak symmetry is broken. The current world-average measured value is $M_W = 80.399 \pm 0.025$ GeV [1] from a combination of measurements from the ALEPH [2], DELPHI [3], L3 [4], OPAL [5], D0 [6], and CDF [7, 8] collaborations.

In this Letter we present a measurement of M_W using data collected from 2002 to 2006 with the D0 detector [9], corresponding to a total integrated luminosity of $1~\text{fb}^{-1}$ [10]. We use the $W \to e\nu$ decay mode because the D0 calorimeter is well-suited for a precise measure-

ment of electron energies, providing an energy resolution of 3.6% for electrons with an energy of 50 GeV. The components of the initial state total momentum and of the neutrino momentum along the beam direction are unmeasurable, so M_W is measured using three kinematic variables measured in the plane perpendicular to the beam direction: the transverse mass m_T, the electron transverse momentum p_T^e, and the neutrino transverse momentum p_T^ν. The transverse mass is defined as $m_T = \sqrt{2p_T^e p_T^\nu (1 - \cos \Delta\phi)}$, where $\Delta\phi$ is the opening angle between the electron and neutrino momenta in the plane transverse to the beam. The magnitude and direction of p_T^ν are inferred from the event missing transverse energy ($\not{E}_T$). The M_W measurement is made by comparing data spectra of m_T, p_T^e, and $\not{E}_T$ with probability density functions (templates) for these spectra constructed from Monte Carlo simulation with varying input M_W values.

The D0 detector [9] contains tracking, calorimeter, and muon systems. Silicon microstrip tracking detectors (SMT) near the interaction point cover pseudorapidity $|\eta| \lesssim 3$ to provide tracking and vertex information. The central fiber tracker surrounds the SMT, providing coverage to $|\eta| \approx 2$. A 2 T solenoid surrounds these tracking detectors. Three uranium, liquid-argon calorimeters measure particle energies. The central calorimeter (CC) covers $|\eta| < 1.1$, and two end calorimeters (EC) extend coverage to $|\eta| \approx 4$. The CC is segmented in depth into eight layers. The first four layers are used primarily to measure the energy of photons and electrons and are collectively called the electromagnetic (EM) calorimeter. The remaining four layers, along with the first four, are used to measure the energy of hadrons. Intercryostat detectors (ICD) provide added sampling in the region $1.1 < |\eta| < 1.4$ where the CC and EC cryostat walls degrade the calorimeter energy resolution. A three level trigger system selects events for recording with a rate of 100 Hz.

Events are initially selected using a trigger requiring at least one EM cluster found in the CC with transverse energy threshold varying from 20 GeV to 25 GeV depending on run conditions. Additionally, the position of the reconstructed production point of a W or Z boson along the beam line is required to be within 60 cm of the center of the detector.

Candidate W boson events are required to have one EM cluster reconstructed in the CC, with $p_T^e > 25$ GeV and $|\eta| < 1.05$ where η is the pseudorapidity measured with respect to the center of the detector. The EM cluster must pass electron shower shape and energy isolation requirements in the calorimeter, be within the central 80% of the electromagnetic section of each CC module, and have one track matching in (η, ϕ) space, where the track has at least one SMT hit and $p_T > 10$ GeV. The central 80% requirement is applied to the ϕ coordinate only and excludes regions with slightly degraded energy resolution. The event must satisfy $\not{E}_T > 25$ GeV, $u_T < 15$ GeV, and $50 < m_T < 200$ GeV. Here $\not{E}_T$ is the magnitude of the vector sum of the transverse energy of calorimeter cells above read out threshold, excluding those in the coarse hadronic layer and in the inter–cryostat detector, and u_T is the magnitude of the vector sum of the transverse component of the energies measured in calorimeter cells excluding those associated with the reconstructed electron. This selection yields 499,830 candidate $W \to e\nu$ events. Throughout this Letter we use "electron" to imply either electron or positron.

We use $Z \to ee$ events for calibration. Candidate Z boson events are required to have two EM clusters satisfying the requirements above. Both electrons must have $p_T^e > 25$ GeV. One must be reconstructed in the CC and the other in either the CC or EC ($1.5 < |\eta| < 2.5$). The associated tracks must be of opposite charge. Events must also have $u_T < 15$ GeV and $70 \text{ GeV} \leq m_{ee} \leq 110 \text{ GeV}$, where m_{ee} is the invariant mass of the dielectron pair. Events with both electrons in the CC are used to determine the EM calibration. There are 18,725 candidate $Z \to ee$ events in this category.

The backgrounds in the W boson sample are $Z \to ee$ events in which one electron escapes detection, multi-jet events (MJ) in which a jet is misidentified as an electron with $\not{E}_T$ arising from misreconstruction, and $W \to \tau\nu \to e\nu\nu\nu$ events. The background from Z boson events arises from electrons which traverse the gap between the CC and EC. The tracking efficiency in this region is high, so this background is estimated by selecting data events passing the W boson selection in which an additional track is pointing at the gap region. The MJ background is determined using a sample obtained by removing the track matching requirement for the electron candidates. The probabilities for background and W boson signal events in this sample to have a matching track are measured in control samples. The number of events in the sample without the track requirement and the two probabilities are then used to determine the number of MJ background events in the final W boson sample. The $W \to \tau\nu \to e\nu\nu\nu$ contribution is determined from detailed simulation of the process using the D0 GEANT [11]-based simulation. The backgrounds expressed as a fraction of the final sample are $(0.80 \pm 0.01)\%$ from $Z \to ee$, $(1.49 \pm 0.03)\%$ from MJ, and $(1.60 \pm 0.02)\%$ from $W \to \tau\nu \to e\nu\nu\nu$.

W and Z boson production and decay kinematics are simulated using the RESBOS [12] next-to-leading order generator which includes non-perturbative effects at low boson p_T. These effects are parametrized by three constants (g_1, g_2 and g_3) whose values are taken from global fits to data [13]. The radiation of one or two photons is performed using the PHOTOS [14] program.

Detector efficiencies and energy response and resolution for the electron and hadronic energy are applied

to the RESBOS+PHOTOS events using a fast parametric Monte Carlo simulation (FASTMC) developed for this analysis. The FASTMC parameters are determined using a combination of detailed simulation and control data samples. The primary control sample used for both the electromagnetic and hadronic response tuning is $Z \to ee$ events. W boson events are also used in a limited manner, as are events recorded in random beam crossings, with or without requiring hits in the luminosity counters.

Since the Z boson mass and width are known with high precision from measurements [15] at the CERN e^+e^- collider (LEP), these values are used to calibrate the electromagnetic calorimeter response assuming a form $E^{\mathrm{meas}} = \alpha\, E^{\mathrm{true}} + \beta$ with α and β constants determined by calibration. The M_W measurement is effectively a measurement of the ratio of W and Z boson masses. Figure 1 shows a comparison of the m_{ee} distributions for data and FASTMC, as well as the χ distribution defined as the difference between data and the FASTMC prediction divided by the statistical uncertainty on the difference.

The other major calibration is that of the hadronic energy in the event, which includes energy recoiling against the boson. The hadronic response (resolution) is tuned using the mean (width) of the η_{imb} distribution in $Z \to ee$ events in bins of p_T^{ee}. Here η_{imb} is defined as the sum of the projections of the dielectron momentum ($\vec{p}_T^{\,ee}$) and $\vec{u}_T$ vectors in the transverse plane on the axis bisecting the dielectron opening angle [16].
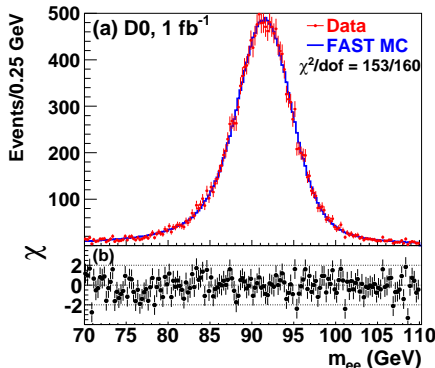

FIG. 1: (a) The dielectron invariant mass distribution in $Z \to ee$ data and from the fast simulation FASTMC and (b) the χ values where $\chi_i = (N_i - \mathrm{FASTMC}_i)/\sigma_i$ for each point in the distribution, N_i is the data yield in bin i and only the statistical uncertainty is used. The fit range is indicated by the double-ended horizontal arrow.

To determine M_W, FASTMC template distributions for m_T, p_T^e, and $\not{\!\!E}_T$ are generated at a series of test M_W values at intervals of 10 MeV with the backgrounds added to the simulated distributions. A binned likelihood between the data and each template is then computed. The resulting log likelihoods as a function of mass are fit to a parabola. The minimum point of the parabola defines the measured M_W value. The fits are performed separately for each of the m_T, p_T^e, and $\not{\!\!E}_T$ distributions, and the fit ranges were chosen to minimize the total expected uncertainty on M_W for each distribution.

A test of the analysis procedure is performed using events produced by the detailed GEANT Monte Carlo simulation treated as collider data. The methods used for the data analysis are applied to the simulated events, including the FASTMC tuning using the simulated $Z \to ee$ events. Each of the M_W fit results using the m_T, p_T^e, and $\not{\!\!E}_T$ distributions agree with the input M_W value within the 20 MeV total uncertainty of the test.

During the FASTMC tuning for the collider data analysis, M_W returned from fits is blinded by the addition of an unknown constant offset. The same offset was used for m_T, p_T^e and $\not{\!\!E}_T$. This allowed the full tuning on the W and Z boson events and internal consistency checks to be performed without knowledge of the final result. Once the important data and FASTMC comparison plots have acceptable χ distributions, the results are unblinded. The Z boson mass value from the post-tuning fit is 91.185 ± 0.033 (stat) GeV, in agreement with the world average of 91.188 GeV used for the tuning. The M_W results from data after unblinding are given in Table I. The m_T, p_T^e, and $\not{\!\!E}_T$ distributions showing the data and FASTMC template with background for the best fit M_W are shown in Fig. 2.

TABLE I: Results from the fits to data. The uncertainty is only the statistical component.

Variable	Fit Range (GeV)	M_W (GeV)	χ^2/dof
m_T	$65 < m_T < 90$	80.401 ± 0.023	$48/49$
p_T^e	$32 < p_T^e < 48$	80.400 ± 0.027	$39/31$
$\not{\!\!E}_T$	$32 < \not{\!\!E}_T < 48$	80.402 ± 0.023	$32/31$

The systematic uncertainties in the M_W measurement arise from a variety of sources, and can be categorized as those from experimental sources and those from uncertainties in the production mechanism. The systematic uncertainties are summarized in Table II.

The uncertainties on the electron energy calibration and the hadronic recoil model are determined by simultaneously varying the parameters determined in the tuning to $Z \to ee$ events by one statistical standard deviation including correlation coefficients. The electron energy resolution systematic uncertainty is determined by varying resolution parameters determined in the fit to the width of the observed $Z \to ee$ m_{ee} distribution. The shower modeling systematic uncertainties are determined by varying the amount of material representing the detector in the detailed simulation within the uncertainties found by comparing the electron showers in the simulation to those observed in data. The systematic uncertainty for the energy loss differences arising from differing η distributions for the electrons from W and
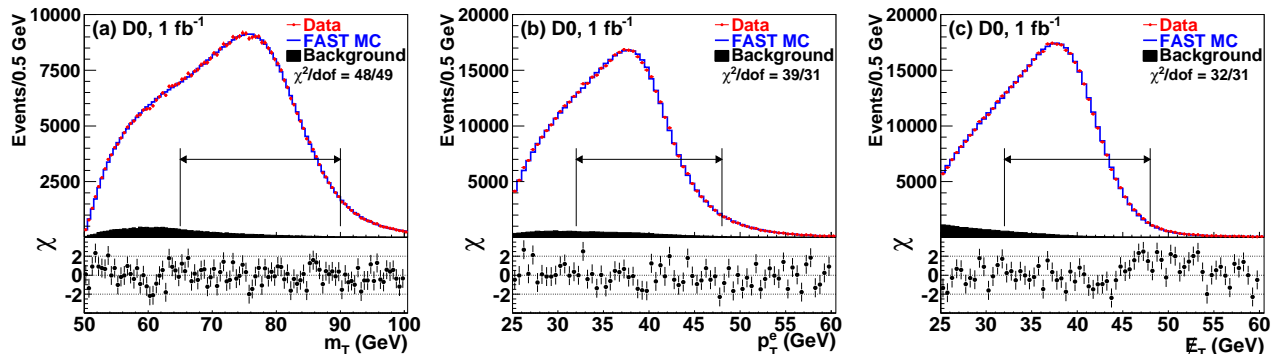
FIG. 2: The (a) m_T, (b) p_T^e, and (c) $\not{E}_T$ distributions for data and FASTMC simulation with backgrounds. The χ values are shown below each distribution where $\chi_i = (N_i - \text{FASTMC}_i)/\sigma_i$ for each point in the distribution, N_i is the data yield in bin i and only the statistical uncertainty is used. The fit ranges are indicated by the double-ended horizontal arrows.

TABLE II: Systematic uncertainties of the M_W measurement.

	ΔM_W (MeV)		
Source	m_T	p_T^e	$\not{E}_T$
Electron energy calibration	34	34	34
Electron resolution model	2	2	3
Electron shower modeling	4	6	7
Electron energy loss model	4	4	4
Hadronic recoil model	6	12	20
Electron efficiencies	5	6	5
Backgrounds	2	5	4
Experimental Subtotal	35	37	41
PDF	10	11	11
QED	7	7	9
Boson p_T	2	5	2
Production Subtotal	12	14	14
Total	37	40	43

Z boson decay is limited by the statistical precision of the simulated test samples. The electron efficiency systematic is determined by varying the efficiency by one standard deviation. The background uncertainties are determined by varying the backgrounds by uncertainties presented earlier.

Among the production uncertainties, the parton distribution function (PDF) uncertainty is determined by generating W boson events with the PYTHIA [17] program using the CTEQ6.1M [18] PDF set. The CTEQ prescription [18] is used to determine a one standard deviation uncertainty [8] on M_W. The QED uncertainty is determined using WGRAD [19] and ZGRAD [20], varying the photon-related parameters and assessing the variation in M_W. The boson p_T uncertainty is determined by varying g_2 by its quoted uncertainty [13]. Variation of g_1 and g_3 has negligible impact.

The quality of the simulation is indicated by the good χ^2 values computed for the difference between the data and FASTMC shown in the figures. The data are also sub-divided into statistically independent categories based on instantaneous luminosity, time, the total hadronic transverse energy in the event, the vector sum of the hadronic energy, and electron pseudorapidity range. The fit ranges are also varied. The results are stable to within the measurement uncertainty for each of these tests.

The results from the three methods have combined statistical and systematic correlation coefficients of 0.83, 0.82, and 0.68 for (m_T, p_T^e), $(m_T, \not{E}_T)$, and $(p_T^e, \not{E}_T)$ respectively. The results are combined [21] including these correlations to give the final result

$$M_W = 80.401 \pm 0.021 \text{ (stat)} \pm 0.038 \text{ (syst) GeV}$$
$$= 80.401 \pm 0.043 \text{ GeV}.$$

The dominant uncertainties arise from the available statistics of the $W \to e\nu$ and $Z \to ee$ samples. Thus, this measurement can still be expected to improve as more data are analyzed by the D0 experiment. The M_W measurement reported here agrees with the world average and the individual measurements and is more precise than any other single measurement. Its introduction in global electroweak fits is expected to lower the upper bound on the SM Higgs mass, although it is not expected to change the best fit value [1].

[a] Visitor from Augustana College, Sioux Falls, SD, USA.
[b] Visitor from Rutgers University, Piscataway, NJ, USA.
[c] Visitor from The University of Liverpool, Liverpool, UK.
[d] Visitor from Centro de Investigacion en Computacion - IPN, Mexico City, Mexico.
[e] Visitor from ECFM, Universidad Autonoma de Sinaloa, Culiacán, Mexico.
[f] Visitor from Universität Bern, Bern, Switzerland.
[g] Visitor from Universität Zürich, Zürich, Switzerland.

[1] The LEP Electroweak Working Group, CERN-PH-EP/2008-20, arXiv:0811.4682 [hep-ex] (2008), and The Tevatron Electroweak Working Group, FERMILAB-TM-2415 (2008). More information is available at: http://tevewwg.fnal.gov.
[2] S. Schael et al. (ALEPH Collaboration), Eur. Phys. J. C 47, 309 (2006).
[3] J. Abdallah et al. (DELPHI Collaboration), Eur. Phys. J. C 55, 1 (2008).
[4] P. Achard et al. (L3 Collaboration), Eur. Phys. J. C 45, 569 (2006).
[5] G. Abbiendi et al. (OPAL Collaboration), Eur. Phys. J. C 45, 307 (2006).
[6] B. Abbott et al. (D0 Collaboration), Phys. Rev. D 58, 092003 (1998); B. Abbott et al. (D0 Collaboration), Phys. Rev. D 62, 092006 (2000); V. M. Abazov et al. (D0 Collaboration), Phys. Rev. D 66, 012001 (2002).
[7] T. Affolder et al. (CDF Collaboration), Phys. Rev. D 64, 052001 (2001).
[8] T. Aaltonen et al. (CDF Collaboration), Phys. Rev. Lett. 99, 151801 (2007); T. Aaltonen et al. (CDF Collaboration), Phys. Rev. D 77, 112001 (2008).
[9] V. M. Abazov et al. (D0 Collaboration), Nucl. Instrum. Methods in Phys. Res. A 565, 463 (2006).
[10] T. Andeen et al., FERMILAB-TM-2365 (2007).
[11] R. Brun and F. Carminati, CERN Program Library Long Writeup W5013 (1993).
[12] C. Balazs and C.P. Yuan, Phys. Rev. D 56, 5558 (1997).
[13] F. Landry, R. Brock, P. Nadosky, and C.P. Yuan, Phys. Rev. D 67, 073016 (2003).
[14] E. Barbiero and Z. Was, Comput. Phys. Commun. 79, 291 (1994).
[15] C. Amsler et al., Phys. Lett. B 667, 1 (2008) and references therein.
[16] J. Alitti et al. (UA2 Collaboration), Phys. Lett. B 276, 354 (1992).
[17] T. Sjöstrand et al., Comput. Phys. Commun. 135, 238 (2001).
[18] H.L. Lai et al., Phys. Rev. D 55, 1280 (1997); J. Pumplin et al., JHEP 0310, 046 (2003).
[19] U. Baur et al., Phys. Rev. D 59, 013002 (1999).
[20] U. Baur et al., Phys. Rev. D 57, 199 (1998); U. Baur et al., Phys. Rev. D 65, 033007 (2002).
[21] L. Lyons, D. Gibout, and P. Clifford, Nucl. Instrum. Methods in Phys. Res. A 270, 110 (1988); A. Valassi, Nucl. Instrum. Methods in Phys. Res. A 500, 391 (2003).